Cell, Vol. 91, 961–971, December 26, 1997, Copyright ©1997 by Cell Press

The Structural Basis for 14-3-3:Phosphopeptide Binding Specificity

Michael B. Yaffe,[1,2,7] Katrin Rittinger,[5] Stefano Volinia,[1] Paul R. Caron,[4] Alastair Aitken,[5] Henrik Leffers,[6] Steven J. Gamblin,[5] Stephen J. Smerdon,[5] and Lewis C. Cantley[1,3]

[1]Division of Signal Transduction
Department of Medicine
[2]Department of Surgery
Beth Israel Deaconess Medical Center
Boston, Massachusetts 02215
[3]Department of Cell Biology
Harvard Medical School
Boston, Massachusetts 02115
[4]Vertex Pharmaceuticals
130 Waverly Street
Cambridge, Massachusetts 02139
[5]Division of Protein Structure
National Institute for Medical Research
Mill Hill, London, NW 7 1AA
United Kingdom
[6]Department of Growth and Reproduction
Section GR-5064, Rigshospitalet
Blegdamsvej 9 DK-2100 Copenhagen
Denmark

Summary

The 14-3-3 family of proteins mediates signal transduction by binding to phosphoserine-containing proteins. Using phosphoserine-oriented peptide libraries to probe all mammalian and yeast 14-3-3s, we identified two different binding motifs, RSXpSXP and RXY/FXpSXP, present in nearly all known 14-3-3 binding proteins. The crystal structure of 14-3-3ζ complexed with the phosphoserine motif in polyoma middle-T was determined to 2.6 Å resolution. The bound peptide is in an extended conformation, with a tight turn created by the pS +2 Pro in a *cis* conformation. Sites of peptide–protein interaction in the complex rationalize the peptide library results. Finally, we show that the 14-3-3 dimer binds tightly to single molecules containing tandem repeats of phosphoserine motifs, implicating bidentate association as a signaling mechanism with molecules such as Raf, BAD, and Cbl.

Introduction

14-3-3 proteins constitute a highly conserved family of homo- and heterodimeric molecules present in high abundance in all eukaryotic cells (Aitken, 1996). There are at least seven distinct genes for 14-3-3 in vertebrates, giving rise to nine isotypes (α,β,γ,δ,ϵ,η,σ,τ, and ζ, with α and δ being phosphorylated forms of β and ζ, respectively) (Aitken et al., 1995a). Recent findings have implicated 14-3-3 as a key regulator of signal transduction events. Through interacting with Cdc25C, 14-3-3 regulates entry into the cell cycle (Peng et al., 1997); 14-3-3 interacts with BAD preventing apoptosis by releasing Bcl-X_L (Zha et al., 1996), and 14-3-3 regulates Raf signaling in a manner that is complex and poorly understood (c.f. Freed et al., 1994; Fu et al., 1994; Irie et al., 1994). In addition, 14-3-3 proteins interact with other signaling molecules including members of the protein kinase C family (Toker et al., 1990; Meller et al., 1996), Cbl (Liu et al., 1996), IRS1 (Craparo et al., 1997), and polyoma middle-T antigen (Pallas et al., 1994).

A major advance in understanding 14-3-3 function was the recognition by Muslin et al. (1996) that 14-3-3's interaction with c-Raf was mediated by direct binding to phosphoserine. Similar phosphorylation-dependent interactions with 14-3-3 have now been clearly demonstrated for Cbl (Liu et al., 1997), nitrate reductase (Moorhead et al., 1996), BAD (Zha et al., 1996), the epithelial keratins K8/18 (Liao and Omary, 1996), Cdc25C (Peng et al., 1997), and the IGF-1 receptor (Craparo et al., 1997). Using peptides derived from c-Raf, Muslin et al. (1996) identified the motif RSXpSXP as important for high affinity 14-3-3 binding. While several 14-3-3 target proteins contain exact matches to this motif, an approximately equal number do not, indicating that additional sequences also allow phosphoserine-dependent 14-3-3 binding. Intriguingly, phosphoserine-dependent interactions between target proteins and the 14-3-3 dimer are reminiscent of the phosphotyrosine-dependent assembly of signaling complexes mediated by SH2 and PTB domains.

Crystal structures of both the τ and ζ isotypes of 14-3-3 have been determined (Liu et al., 1995; Xiao et al., 1995), and these highly similar structures show each monomer within the dimer to be composed of nine antiparallel α helices. These structures were solved in the absence of a phosphopeptide ligand, hence the structural basis for 14-3-3 binding to target proteins was unclear. To address these issues, we used a degenerate phosphoserine-oriented peptide library technique to examine the sequence requirements for binding to 14-3-3. This approach identified two different motifs, one of which corresponds closely to the that originally deduced by Muslin et al. (1996). Equilibrium binding experiments using synthetic peptides confirmed these findings. When the peptide library screening results were used to scan mammalian sequences in the SWISS-PROT data bank, we identified many known and several novel proteins as putative 14-3-3 binding partners.

These data were then used to select peptide sequences for cocrystallization with 14-3-3. We report here the crystal structure of 14-3-3ζ in complex with a phosphoserine peptide containing the binding motif of polyoma middle-T (mT). The structure shows that the peptide binds to 14-3-3 in an extended conformation with a tight turn toward its C terminus generated by a *cis*-proline residue. It identifies the residues involved in coordinating the serine phosphate and provides a molecular explanation for our peptide library results and for the site-directed mutational data reported by others. We also

[7]To whom correspondence should be addressed at Beth Israel Deaconess Medical Center, HIM 1018, 330 Brookline Avenue, Boston, Massachusetts 02215.

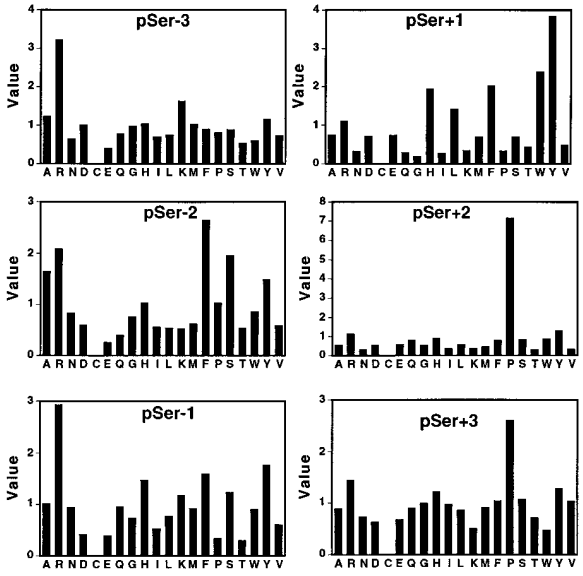

Figure 1. Substrate Specificity for 14-3-3τ

A phosphoserine-oriented degenerate peptide library of general sequence MAXXXpSXXXAKK, where X indicates any amino acid except Cys, was used to screen Human 14-3-3τ. Approximately 1 mg of a 14-3-3 τ-MBP fusion protein bound to amylose beads was incubated with 1.2 mg of the peptide library. Following extensive washing, bound peptides were eluted and sequenced. Each panel shows the relative abundance of each of the 19 amino acids at a given cycle of sequencing compared to their abundance in the starting library mixture. The one-letter amino acid code listed in Table 1 is used.

demonstrate that the 14-3-3 dimer binds with very high affinity to a peptide containing two phosphoserine motifs, suggesting that proteins with two tandem phosphoserine motifs (e.g., Raf) could be trapped in a very high affinity complex through a bidentate association with the 14-3-3 dimer.

Results

Peptide Libraries Define Two Distinct Motifs for 14-3-3 Binding

We investigated the binding of a series of phosphoserine-oriented degenerate peptide libraries to all mammalian 14-3-3 isotypes (with the exception of γ) and to both Saccharomyces cerevisiae 14-3-3 gene products using the technique of Songyang et al. (1993). Figure 1 shows results for the τ isoform, using a library containing a fixed phosphoserine residue (pS) flanked by three degenerate positions on each side. (Residues are numbered according to their proximity to the phosphoserine [pS] and negative if they are located N-terminal to it.) 14-3-3τ showed strong selection for peptides containing Arg or Lys in the pS −3 position; Phe, Tyr, Ser, or Arg in the pS −2 position; basic residues in the pS −1 position; and aromatic residues or Leu in the pS +1 position. There was extremely strong selection for peptides with Pro in the pS +2 position. The pS +3 position was also high in Pro, but this was in part due to carry-over from the previous sequencing cycle. All 14-3-3 isotypes investigated, including both yeast isotypes, selected the same motif (data not shown), despite the reported isotype-specific differences in 14-3-3:target protein interactions (c.f. Aitken et al., 1995b; Meller et al., 1996; Vincenz and Dixit, 1996).

To test and extend this motif, a second phosphoserine-oriented library was constructed incorporating a fixed Pro residue in the pS +2 position and extending the degeneracy to four residues on either side of the phosphoserine. All 14-3-3 isotypes strongly selected for peptides with Arg in the pS −4 position (Table 1), with preference values generally exceeding 4, approximately 1.7-fold higher than those observed for Arg in the pS −3 position. Selection for residues at the other sites agreed well with the results from the initial phosphoserine library, namely selection for peptides containing Arg or Lys in the pS −3 position; Ser, Phe, or Tyr in the pS −2 position, basic residues in the pS −1 position, and aromatic or aliphatic residues in the pS +1 position. No additional selection was observed for residues C-terminal to the Pro in the pS +2 position. Ser was slightly preferred over aromatic amino acids in the pS −2 position using this library, while the reverse was true for the first library tested. Both yeast 14-3-3 isoforms (Bmh1 and Bmh2) showed additional selection for His and Ala in the pS −2 position.

Two additional degenerate peptide libraries were constructed to clarify the amino-terminal portion of the 14-3-3 binding motif. Based on the results in Table 1, a pSer-Xxx-Pro degenerate library was constructed containing Arg residues fixed in both the pS −4 and pS −1 positions, and extending the region of sequence degeneracy to seven positions N-terminal to the pS residue (Table 2). An Arg residue in the pS −4 position removed the requirement for a positively charged side-chain in the pS −3 position, leading instead to slight preference for Leu or Met. There was little additional amino acid selection, other than a slight preference for Arg, in positions further upstream than pS −4, demonstrating that 14-3-3:peptide interaction spans four residues N-terminal to, and two residues C-terminal to, the peptide's phosphoserine position. Trp and Thr, along with Phe, Tyr, and Ser were selected in the pS −2 position. For most of the 14-3-3 isotypes, placement of an Arg in the pS −4 position led to a preference for aromatic residues over Ser/Thr in the pS −2 position (see below). In addition, selection for Leu, Ala, Glu, and Met in the pS +1 position became evident.

When 14-3-3 isotypes were probed using a pSer-Xxx-Pro library containing an Arg residue fixed in the pS −3 position, a slightly different motif emerged (Table 2). All 14-3-3 isotypes selected additional Arg or Lys residues in the pS −4 position, suggesting that a positive charge in the pS −4 position dominates over the pS −3 position. In addition, Arg in the pS −3 position led all 14-3-3 isotypes to select for Ser over aromatic residues at pS −2, in contrast to having Arg fixed in the pS −4 position (Table 2). Basic residues, particularly His, were still preferred at the pS −1 position, although both Sigma and Bmh1 isotypes of 14-3-3 also selected for aromatic residues (data not shown). Preference for Leu, Ala, Glu,

Table 1. Refinement of Substrate Specificities for 14-3-3

	Position								
Isotype	−4	−3	−2	−1	pSer	+1	Pro	+3	+4
Beta	**R** (4.3)	**R** (2.6) K (1.3)	**F** (2.1) **S** (2.0) **Y** (1.7) W (1.4)	**R** (2.1) **H** (2.0) K (1.3)	pSer	**W** (2.9) **Y** (2.1) **F** (1.7) **L** (1.7)	P	X	X
Eta	**R** (2.2)	**K** (1.5)	**S** (2.3) **F** (2.0) **Y** (1.6)	**R** (1.8) **H** (1.6) K (1.3)	pSer	**W** (2.1) **Y** (1.9) **L** (1.8) **A** (1.7) **F** (1.6)	P	X	X
Epsilon	**R** (4.4)	**R** (3.2) K (1.4)	**S** (2.0) **Y** (1.9) **F** (1.9)	**R** (2.1) **H** (1.8) K (1.3)	pSer	**W** (2.2) **Y** (2.1) **L** (2.0) **A** (1.7) **F** (1.6)	P	X	X
Sigma	**R** (4.9)	**R** (3.4) K (1.2)	S (1.5) F (1.5) Y (1.4)	**R** (2.9) H (1.5) K (1.3)	pSer	**Y** (2.8) **W** (2.3) **F** (2.0) L (1.4)	P	X	X
Tau	**R** (4.8)	**R** (2.9) K (1.4)	**S** (2.4) **F** (1.7) **Y** (1.6)	**R** (2.1) **H** (1.7) K (1.4)	pSer	**Y** (2.8) **W** (2.3) **F** (2.0) L (1.4)	P	X	X
Zeta	**R** (4.7)	**R** (3.2) K (1.3)	**S** (2.0) **F** (1.8) Y (1.5)	**R** (2.6) **H** (1.7) K (1.3)	pSer	**W** (2.0) **Y** (2.0) **F** (1.7) L (1.4)	P	X	X
Bmh1	**R** (2.5)	**K** (1.6)	**S** (1.9) **F** (1.8) **H** (1.6) A (1.4) Y (1.4)	**H** (2.1) R (1.5) K (1.5)	pSer	**L** (1.9) **A** (1.6) Y (1.5) M (1.5) W (1.3)	P	X	X
Bmh2	**R** (2.0)	K (1.5)	**S** (1.9) **F** (1.8) H (1.5) A (1.4) Y (1.4)	**H** (1.9) K (1.4)	pSer	**L** (1.9) **W** (1.6) **A** (1.6) **M** (1.6) Y (1.5) F (1.4)	P	X	X

14-3-3 specificity deduced through the use of a phospho-Ser-oriented degenerate peptide library. GST- or MBP-fusions of the indicated 14-3-3 isotypes were screened with a peptide library containing the sequence MAXXXXpSXPXXAKK, where X indicates all amino acids except Cys. Selectivity values are shown in parentheses, and values of 1.6 or greater are shown in bold. On the basis of peptide library studies of a variety of other proteins, values of 1.4 or greater denote significant selection, and values greater than 2.0 indicate strong selection. Abbreviations for the amino acid residues are as follows: A, Ala; D, Asp, E, Glu; F, Phe; G, Gly; H, His; I, Ile; L, Leu; M, Met; N, Asn; P, Pro; Q, Gln; R, Arg; S, Ser; T, Thr; V, Val; W, Trp; and Y, Tyr.

and Met in the pS +1 position was maintained. These results suggest that 14-3-3 proteins recognize two different, but related, binding motifs within phosphorylated proteins. One mode uses the optimal motif R-S-[+/Ar]-pS-[L/E/A/M]-P (where Ar indicates an aromatic residue and + indicates a basic residue), similar to the original RSXpSXP motif identified by Muslin et al. (1996). A novel second motif uses the optimal sequence R-X-[Ar]-[+]-pS-[L/E/A/M]-P and has not previously been identified as a 14-3-3 binding motif.

An additional Arg-Ser-Xxx-pSer-Xxx-Xxx library was constructed to investigate the necessity for a Pro residue in the pS +2 position. As shown in Table 2, placement of preferred amino acids N-terminal to the phosphoserine did not alter the strong selection for Pro in the pS +2 position, although Gly was the next best alternative. In addition, this library demonstrated selection for His and other aromatic amino acids along with Gln in the pS −1 position.

Binding Affinities of Optimal Phosphopeptides

To verify the results obtained with the peptide library technique, individual peptides were synthesized and assayed for 14-3-3 binding using surface plasmon resonance (Biacore). Real-time kinetic measurements of 14-3-3 η-GST fusion protein binding to an immobilized 15-mer peptide encompassing the phosphoserine-259 region of c-Raf-1 gave a K_{on} of $2.65 \times 10^4 M^{-1}s^{-1}$, a K_{off} of $3.09 \times 10^{-3}s^{-1}$, and a calculated K_D of 116 nM, in excellent agreement with values reported by Muslin et

Table 2. Multiple Modes of 14-3-3 Binding

Position									
−7	−6	−5	−4	−3	−2	−1	pSer	+1	+2
X	X	X	R	L (1.2) M (1.2)	**Y** (2.0) **F** (1.8) **T** (1.6) W (1.4) S (1.4)	R	pSer	**L** (2.3) **E** (2.2) A (1.4) M (1.4)	P
		X	**K** (1.7) R (1.2)	R	**S** (2.4) **W** (2.0) **F** (1.8) **A** (1.6) Y (1.5) H (1.2)	**H** (1.6) K (1.3) R (1.2)	pSer	**L** (2.3) **E** (1.8) **A** (1.6) M (1.4)	P
				R	S	**Q** (2.0) **Y** (1.7) **F** (1.6) H (1.5) M (1.4)	pSer	**L** (3.1) **M** (1.9) **E** (1.8)	**P** (5.0) G (1.5)

Additional 14-3-3-binding motif refinement was performed using the peptide libraries shown above. Fixed residue positions are indicated by large type, and strongly selected residues are shown in bold. Absolute selectivity values for 14-3-3ζ are shown in parentheses. Results for all other isoforms were similar. Fixing Arg in the pS −4 position selects aromatic residues over Ser in the pS −2 position, in contrast to fixing Arg in the pS −3 position.

al. (1996) using a 14-3-3 ζ-GST fusion. This 15 amino acid peptide uses the mode 1 14-3-3 binding motif homologous to the RSXpSXP sequence originally identified by Muslin et al. (1996) but contains an additional Arg residue in the pS −5 position (Figure 2). Interpretation of this affinity is complicated by the fact that 14-3-3 is a dimer and could simultaneously interact with two phospho-Ser peptides on the chip (see below).

We next investigated preferred residues in the pS −1 and pS +1 positions, using smaller peptides lacking positively charged residues further upstream of the essential RSXSXP motif. Since the small size of these peptides resulted in poor chemical coupling to the sensor chip, a solution-based binding inhibition assay was used (Muslin et al., 1996) (Figure 2, top), which also circumvented potential problems of bidentate binding to immobilized peptides (Experimental Procedures). Plots of initial binding rates as a function of inhibitory peptide concentration gave curves from which the K_Is, corresponding to 50% inhibition of binding, could be determined.

The peptide containing the sequence RSApSEP corresponding to the second 14-3-3 binding site in Raf at the Ser-621 phosphorylation site gave a K_I of 1270 nM, 2.5-fold higher than for the pS-Raf-259 peptide in solution, which gave a K_I of 510 nM. The Raf-621 peptide contains a preferred Glu in the pS +1 position, but lacks the additional positive charge upstream from the Arg in the pS −3 position, present in the pS-Raf-259 peptide. In contrast, a peptide containing the sequence RSHpSYP corresponding to the 14-3-3 binding site in mT had a K_I of 435 nM. This peptide, which contains both a preferred His residue in the pS −1 site and a Tyr residue in the pS +1 site, binds even more tightly than the pS-Raf-259 peptide, despite lacking additional basic residues upstream from the pS −3 position. This result verifies the importance of amino acid residues in the pS −1 and pS +1 positions selected using the peptide library technique. A variant of this peptide lacking the pS −3 Arg (sequence ASHpSYP) had a K_I of 1400 nM, confirming the importance of basic residues in this position (data not shown).

A nonphosphorylated analog of the Raf-259 peptide was unable to inhibit 14-3-3 binding to the sensor chip at peptide concentrations up to 50 μM. Consequently, phosphorylation of Ser (and presumably Thr) residues seems essential for 14-3-3 binding.

Next, peptides containing optimized sequences for mode 2 binding were investigated. Peptides containing Arg in the pS −4 position rather than the pS −3 position, His in the pS −1 position, and Leu in the pS +1 position were synthesized with amino-terminal glycine linkers, biotinylated, and bound to Streptavidin-coated Biacore sensor chips to measure directly 14-3-3 binding kinetics (Figure 2, bottom). The peptide RLSHpSLP bound tightly to 14-3-3, giving a K_D of 55.7 nM. This value is more than 3-fold higher than that calculated for the highly homologous RSHpSYP peptide from mT, where the Arg residue is in the pS −3, rather than pS −4 position, in agreement with preference for a positive charge in the pS −4 site determined by the peptide library (Table 2). When Ser in the pS −2 position was replaced by a Tyr residue (RLYHpSLP), the binding improved by another 33%, giving a K_D of 37.4 nM. This finding agrees with the predicted mode 2 binding, which prefers peptides with Arg in the pS −4 position and aromatic residues in the pS −2 site. Replacing the Pro in the pS +2 position in the original peptide by Gly reduced the binding approximately 4-fold, giving a K_D of 190 nM (Figure 2), again in agreement with the peptide library results (Table 2). The kinetic constants for all three peptides revealed that the major effect of these amino acid substitutions was modulation of the off-rate. The on-rate for all three peptides was similar (Figure 2). The same rank order of binding was observed when mode 2 peptides were assayed using the solution-inhibition assay (data not shown).

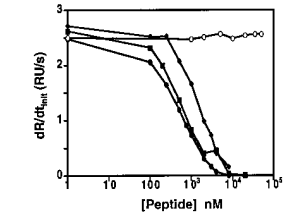

Peptide	Sequence	K_I (nM)
pS-raf 259	RSRST*p*STP	510
pS-raf 621	RSA*p*SEP	1270
pS-mT	RSH*p*SYP	435
raf 259	RSRSTSTP	> 50,000

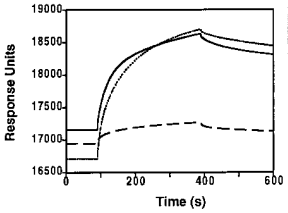

Sequence	K_{off} s^{-1} (x 10^{-3})	K_{on} M^{-1} s^{-1} ($x10^4$)	K_D nM
RLSH*p*SLP	2.05	3.68	55.7
RLYH*p*SLP	1.08	2.89	37.4
RLSH*p*SLG	6.99	3.67	190.4

Figure 2. Peptide Binding to 14-3-3: Kinetic and Inhibition Analyses Using Surface Plasmon Resonance (Biacore)

(Top) Solution inhibition assay for mode 1 peptides from c-raf-1 and polyoma middle-T. 14-3-3 η-GST fusion protein (200 nM) was incubated with increasing amounts of each of the indicated peptides for 1 hr at 23°C, then infused over a sensor chip prederivitized with an excess of the ps-raf 259 peptide. (Closed circle) pS-mT peptide; (closed square) pS-raf 259 peptide; (closed diamond) ps-raf 621 peptide; (open circle) unphosphorylated raf-259 peptide. The initial rate of binding, dR/dt_{init}, which indicates the amount of 14-3-3 not complexed to the inhibitor peptides, was measured and K_Is corresponding to a 50% reduction in dR/dt_{init} determined.

(Bottom) Binding of 14-3-3 η-GST to immobilized mode 2 peptides. Peptides corresponding to optimal sequences for mode 2 binding were synthesized with the biotinylated N-terminal linker Met-Ala-$(Gly)_3$-, bound to a strepatavidin-coated sensor chip, and analyzed for 14-3-3 binding. Sensorgrams for peptide sequences RLSH*p*SLP (solid line), RLYH*p*SLP (dotted line), and RLSH*p*SLG (dashed line) are shown, with 14-3-3-GST concentration 500 nM, flow rate 10 μl/min. Association and dissociation phases over a wide range of 14-3-3 concentrations for each peptide were analyzed, and the on- and off-rates for binding determined. The measured on-rates were found to be similar for all three peptides, in contrast to significant sequence-dependent variations in K_{off}.

The Crystal Structure of 14-3-3ζ Complexed to a Phosphoserine Peptide

Additional refinement of the previously reported 14-3-3τ crystal structure (Xiao et al. 1995) revealed a sulfate ion in a basic pocket located on each monomer (Figure 3). The 14-3-3 dimer creates a large channel approximately 35 Å broad, 35 Å wide, and 20 Å deep. The residues that line this channel are largely invariant whereas the more variable residues are distributed on the outer surface. The channel floor is made up of helices A, C, and E from both monomers, while each wall of the channel is made up from helices G and I (Figure 3A). The protein is highly acidic (pI ≈ 4.6), with a cluster of basic residues in the channel forming the sulfate binding pocket (Figure 3B). This site, located at each edge of the channel, is formed by Lys-49, Arg-56, Arg-127, and Tyr-128 located on helices C and E (Figure 3C). The presence of this sulfate ion in the structure, resulting from Li_2SO_4 in the crystallization experiments, suggested the location of the phosphoserine binding pocket.

The crystal structure of 14-3-3ζ complexed to a mode 1 phosphopeptide based on the sequence around Ser-276 in mT (sequence MARSHpSYPAKK) was solved at 2.6 Å resolution by molecular replacement. Initial electron density maps were of good quality and showed strong electron density corresponding to the bound peptide, in both monomeric subunits of the 14-3-3 dimer prior to any inclusion of the peptide in the atomic coordinates used for calculation of structure factor phases. The structure of the complex shows that the bound peptide adopts an extended main chain conformation (Figures 4A and 4B) and is situated at either edge of the conserved channel of the 14-3-3 dimer (Figure 4C). Phosphoserine coordination includes salt bridges to the the side chains of Arg-56, Arg-127, and Lys-49, and a hydrogen bond to the hydroxyl group of Tyr-128 (Figure 4B), mimicking the coordination of the sulfate ions in the unliganded structure (Figure 3C). In the complex, Arg-60 adjoins the basic pocket but does not interact directly with the pSer phosphate. These data are consistent with the site-directed mutation studies of Zhang et al. (1997), where replacement of either Arg-56 or Lys-49 by a Glu significantly affected ligand binding, whereas the equivalent mutation of Arg-60 had only minor effects.

Currently there is no electron density for the guanidinium group of the Arg at pS −3, although there is some weak electron density corresponding to the aliphatic portion of the side chain. This residue is not well ordered, probably as the result of multiple acidic residues in its general vicinity available for potential interactions (Figure 4D); this would both explain the selectivity for Arg or Lys in the peptide library and binding experiments, and our inability to precisely locate the side chain. The Ser side chain in the pS −2 position hydrogen bonds to the pyrrole nitrogen of Trp-228. The main-chain amide of His at pS −1 hydrogen bonds with the side-chain carbonyl of Asn-224. The Tyr ring at pS +1 sits within a hydrophobic pocket that includes Ile-217, Leu-216, and Leu-220, and its hydroxyl probably forms a hydrogen bond with the side chain of Asp-213.

The Pro residue at pS +2 clearly adopts a *cis*-conformation, allowing the ε-amino group of Lys-120 to form a hydrogen bond with the carbonyl oxygen from the pS +1 Tyr that forms one end of the *cis*-Pro imide bond. The aliphatic portion of the pS +2 Pro side chain itself abuts the aliphatic part of the Lys-49 side chain. These interactions produce a sharp change in chain direction, allowing the remaining portions of the peptide to exit the binding cleft (Figure 4). The finding that the Pro at pS +2 adopts a *cis*-conformation provides a powerful rationale for the peptide library results, which show very strong preference for Pro in this position, since the *cis-trans* free energy difference and isomerization barrier for Pro is significantly lower than for any other amino acid (Schulz and Schirmer, 1979). It will be intriguing to see if proteins containing this motif have *cis*-Pro prior to formation of the phosphoserine-mediated complex.

High Affinity Binding to a Doubly Phosphorylated Peptide

Several 14-3-3 binding proteins, including c-Raf-1 and Cbl, contain two 14-3-3 binding sequences separated by polypeptide segments of various lengths. Intriguingly, native 14-3-3 is a dimeric molecule, with the individual monomeric subunits related by a C_2 rotation axis perpendicular to the substrate binding cleft (Figures 3A and 4C),

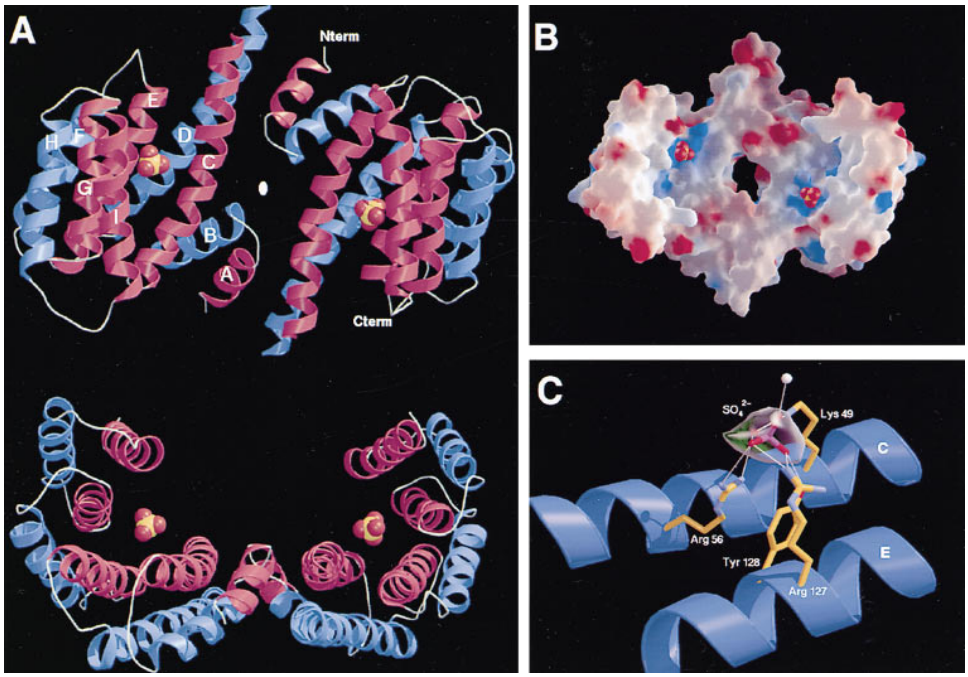

Figure 3. Structure of the 14–4–4 τ Dimer with Bound Sulfate Ion

(A and B) Two orthogonal RIBBONS representations (Carson, 1991) of the 14-3-3τ dimer (A). The sulfate ion, identified after further refinement of the τ structure, is shown in a space-filling representation. Helices lining the invariant inner surface of the large channel are colored in red, whereas helices on the outside of the dimer are colored in blue. Dyad axis is shown in white. The bottom figure is a 90° rotation of the upper figure about the horizontal axis. (The figure was made using Bobscript [Esnouf, 1997] and Raster3D [Merritt and Murphy, 1994]). (B) Electrostatic potential of the 14-3-3 dimer surface calculated using GRASP (Nicholls et al., 1991) and viewed from the same direction as in (A) (top). Negative potential is colored red and positive potential, blue. The bound sulfate ion is shown in a space-filling representation. Helix I has been removed to facilitate visualization of the SO_4 binding site.

(C) The sulfate ion, shown in red and magenta, is coordinated by Lys-49, Arg-56, Arg-127, and Tyr-128. Side chains are shown with carbon atoms colored yellow, oxygen atoms in red, and nitrogen atoms in blue, respectively. A portion of the (F_o-F_c) omit electron density map shown as a transparent surface is contoured at three times the rms density. (The figure made using Bobscript [Esnouf, 1997] and Raster3D [Merritt and Murphy, 1994].)

suggesting important implications for 14-3-3 function in molecules containing tandem 14-3-3 binding motifs. The pSer binding pockets lie 17 Å apart in closest dimension, with the binding cleft running in opposite directions in each half of the dimer. This arrangement would allow simultaneous interaction between two tandem 14-3-3 binding sites in a single polypeptide provided that the chain direction was reversed by creation of a loop segment between the two binding motifs (Figure 5A).

To investigate this, an extended polypeptide was constructed, containing either one or two identical potential 14-3-3 binding sites (sequence RSASEP) separated by a ca. 30 Å–long flexible poly-aminohexanoic acid loop spacer. To create a double-motif-containing loop, both 14-3-3-binding RSASEP motifs included phosphoserine residues at the second serine position, whereas a single-motif control loop peptide contained a phosphoserine in only one of the two motifs (Figure 5). The control peptide with only a single 14-3-3 binding site bound with a K_I of 730 nM, in agreement with the K_Is obtained using the Raf phosphopeptides (Figure 2). Remarkably, inclusion of a second 14-3-3 binding motif within the same peptide (i.e., the doubly phosphorylated pS_2 loop peptide) displayed a greater than 30-fold decrease in the K_I to ~20 nM. This result constitutes strong evidence for simultaneous binding at the adjacent 14-3-3 sites to form a high affinity bidentate complex.

Discussion

Using a panel of five phosphoserine-oriented degenerate peptide libraries, we have uncovered two alternative consensus binding sequences for 14-3-3 (Table 3). Within each consensus motif, the amino acid preferences in each position were very similar between all six mammalian and two yeast 14-3-3 isotypes examined.

In contrast to these peptide library experiments, a variety of intracellular signaling proteins seem to demonstrate preferred or specific interactions with particular 14-3-3 isotypes. These include preferential interactions between PKCθ and Cbl with 14-3-3τ in T-cells (Meller et al., 1996; Liu et al., 1997), IGF1-receptor and IRS1 with 14-3-3ε (Craparo et al., 1997), the apoptosis-inhibitor A20 with 14-3-3β (Vincenz and Dixit, 1996), and the glucocorticoid receptor with 14-3-3η (Wakui et al., 1997).

The specificity of 14-3-3:target–protein interactions does not result from different specificity for the phosphopeptide binding motifs but probably arises from contacts made on the variable surface of 14-3-3 outside the binding cleft. Thus, the highly conserved phosphopeptide motifs selected by all 14-3-3 isotypes in our peptide library experiments establish the minimal sequence criteria required for binding. Additional structural constraints then dictate whether the target actually binds, and if so, to which particular isotypes. In addition,

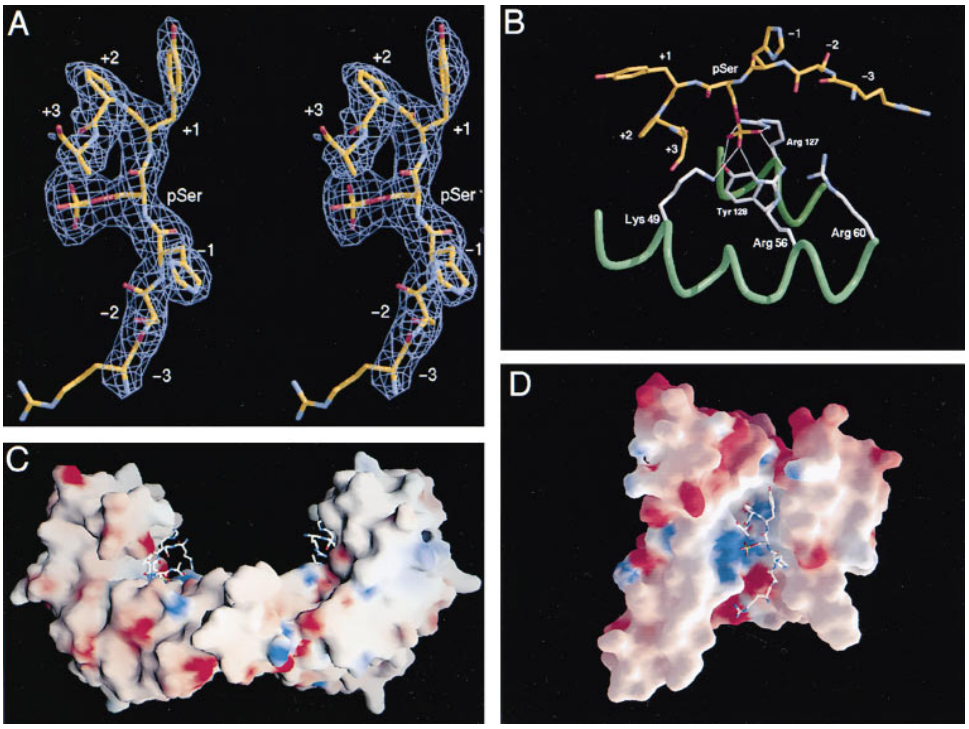

Figure 4. Structure of the 14-3-3ζ:Phosphopeptide Complex

(A) Stereo view of a full atom representation of the phosphopeptide with the (F_o-F_c) omit electron density map, contoured at 3σ, superimposed. Residues N-terminal to the phosphoserine (pSer) are labeled −1 to −3 and those C-terminal are labeled +1 to +3.

(B) Coordination of the phosphate group of the phosphoserine-containing peptide shown with its carbon atoms colored yellow. The phosphate is held by an array of coordinating interactions involving the side-chains of Lys-47 and Arg-56 from helix C and those of Tyr-128 and Arg-127 from helix E. These are each colored with their carbon atoms in gray. This coordination pattern is essentially identical to that observed with the sulfate ion in Figure 3C.

(C) Electrostatic potential surface of the ζ dimer colored as in Figure 3B and seen in end view. The phosphopeptide, in stick representation with oxygen atoms in red and nitrogen atoms in blue superimposed on the ζ surface, sits at each edge of the binding channel in the 14-3-3 dimer.

(D) Electrostatic potential surface of a ζ monomer with superimposed phosphopeptide seen from above. The view is similar to that of the right half of the dimer in Figure 3B.

some of the preferred interactions may be mediated by mass-action effects of tissue-specific expression, since the τ isotype, for example, seems restricted to T cells (Bonnefoy-Berard et al., 1995), and the σ isotype is uniquely expressed in epithelial cells (Leffers et al., 1993). Other interactions may be controlled through the posttranslational phosphorylation of 14-3-3, since the δ-isotype seems to interact more strongly than its non-phosphorylated counterpart ζ (Wheeler-Jones et al., 1996), whereas 14-3-3 phosphorylation seems to impair its ability to bind to c-Raf (Rommel et al., 1996, Dubois et al., 1997).

Our identification of two modes of 14-3-3 binding is reminiscent of the two modes observed for proline-rich peptide-binding to SH3 domains, although in that case the relative N- to C-terminal orientation of the peptides is reversed (Feng et al., 1994; Lim et al., 1994). Whether a similar reversal of peptide orientation occurs between modes for 14-3-3 is not yet known, but it seems unlikely based on the structure determined here.

Liu et al. (1995) have previously proposed that 14-3-3 ligands bind as amphipathic helices; our crystal structure, however, clearly demonstrates that the phosphopeptides bind in an extended conformation. Furthermore, our crystal structure shows how Arg-56 and Lys-49 are involved in coordinating the phosphoserine residue, in excellent agreement with Zhang et al. (1997), where charge reversal at these sites impairs ligand binding. A key feature of our complex structure is the presence of a *cis*-proline in the peptide, which appears necessary to allow the remainder of the peptide to exit the binding cleft. Both residues that are involved in maintaining this conformation, Lys-120 and Lys-49, are conserved in all 14-3-3 isotypes. On the basis of the overall structure of this protein, and the residues surrounding the proline, we do not believe that 14-3-3 has an associated isomerase activity, but rather, that it selectively binds to proteins containing *cis*-prolines within the binding motif. Whether this *cis*-Pro configuration affords an extra level of sophistication in 14-3-3's signaling function remains to be explored.

The structure of the protein:peptide complex rationalizes several additional observations from the peptide library experiments. Selection for Arg/Lys in the pS −3 position and/or Arg in the pS −4 position likely results from the high density of acidic residues near this end of the peptide binding cleft (Figure 4). The region surrounding Trp-228 contains additional hydrophobic amino acids, which might account for selection of aromatic residues along with serine in the pS −2 position. The

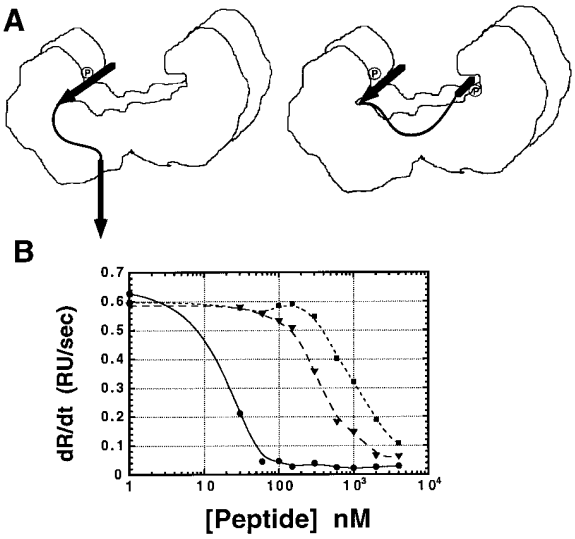

Peptide	Sequence	K_I (nM)
Control	MAGGGGRSA*p*SEP-$_{(AHA)_6}$-RSASEP$_{AKK}$	730
pS_2 Loop	MAGGGGRSA*p*SEP-$_{(AHA)_6}$-RSA*p*SEP$_{AKK}$	~20

Figure 5. Peptides Containing Tandem Phosphoserine Motifs Display Cooperative Binding

(A) A model for cooperative binding of peptides containing one phosphoserine and one serine-containing motif, or two tandem phosphoserine motifs separated by a six–aminohexanoic acid residue bridge to span the binding clefts within a single 14-3-3 dimer. (B) Binding studies using single or tandem phosphoserine motifs using surface plasmon resonance. Increasing amounts of peptides containing a single (control, closed square) or double phosphoserine motif (pS_2 loop, closed circle) were incubated with 14-3-3η-GST protein (120 nM) for 1 hr at 23°C, and assayed for binding using the solution-inhibition assay described in Figure 2A. The ps-Raf-259 peptide (closed triangle) served as an internal control. Incorporating tandem repeats of the 14-3-3 binding motif led to a >30-fold increase in peptide binding affinity.

proximity of Glu-223 to the pS −1 position may account for the selection for basic residues at this site. The strong selection for proline in the pS +2 position presumably results from the relative stability of a *cis* conformation. In a survey of proteins in the Brookhaven Protein Data Bank, Stewart et al. (1990) found that that only 0.05% of Xxx-Xxx amide bonds were *cis* (where Xxx is any amino acid but Pro), in contrast to 6.5% of Xxx-Pro imide bonds. A fuller understanding of the sequence selection criteria revealed by the peptide library experiments awaits the determination of additional 14-3-3:peptide and/or protein complexes. Nevertheless, the residues apparently involved in binding the peptide in our crystal structure, Lys-49, Arg-56, Arg-127, Tyr128, Trp-228, Asn-173, Lys-120, Asn-224, Leu-216, Ile-217, and Leu-220, are conserved in all 14-3-3 isotypes.

Based on the peptide library preference values for all 20 amino acids in flanking positions to a Ser/Thr residue, a weighted screening of all mammalian sequences in the SWISS-PROT database was performed. Separate screens were done using preference values for either mode 1 or mode 2 binding. About 30,000 potential sites were identified in 12,000 protein sequences examined and further evaluated. A variety of potentially important 14-3-3 interacting proteins were identified within the top 5% of highest scores, some of which are listed in Table 3. Many of these are already known to interact with 14-3-3. In addition, several novel target candidates emerged, and additional work will be required to verify or refute whether these proteins do, in fact, bind 14-3-3.

Intriguingly, the 14-3-3 binding motifs, with basic residues 3 or 4 residues N-terminal to phosphorylated Ser, bears strong similarity to the consensus motifs required for PKA, PKC, and PKB/AKT phosphorylation, suggesting these signaling systems have coevolved. In several cases, 14-3-3-binding proteins contain Arg residues in both the pS −4 and pS −3 positions. Since an Arg in the pS −4 position alone is sufficient to confer strong 14-3-3 binding, what is the function of the additional Arg in the pS −3 position? Most likely, this residue is involved in directing phosphorylation of the Ser residue since an Arg in the pS −3 position confers optimal catalytic efficiency for members of the PKC family (Pearson and Kemp, 1991; Nishikawa et al., 1997).

Many proteins have sequences matching several but not all of the residue positions within the optimal consensus motifs (Table 3). Based on our binding data, it appears the closer the sequence match, the tighter the protein binds 14-3-3. The strength of this interaction, in turn, may dictate for a particular target whether 14-3-3 functions as a sequestering protein or as an adaptor.

Two proteins whose sequences best match the mode 1 consensus motif are the polyoma mT antigen and the apoptosis-inducing molecule BAD. mT appears to mimic an activated growth-factor receptor, recruiting a variety of signaling molecules such as src-family kinases, SHC, PP2A, PI 3-kinase, PLC-γ, and hsc70 (Courtneidge and Smith, 1984; Whitman et al., 1985; Campbell et al., 1994, 1995) to result in cell transformation. The optimized 14-3-3 binding motif in mT, RSHpSYP, could ensure that 14-3-3 is available to serve as an adaptor in mT signaling regardless of its interaction with other proteins.

The apoptosis-inducing molecule BAD contains two 14-3-3 binding sites, with sequences RSHpSYP and RSRpSAP. The former is identical to that present in mT, and the latter site is a perfect match to the optimal consensus sequence. Thus, one would predict an extremely tight association between 14-3-3 and BAD, with an extremely slow off-rate. Zha et al. (1996) have shown that 14-3-3 functions by sequestering doubly serine-phosphorylated BAD, preventing it from heterodimerizing with BCL-X_L, and thus, protecting the cell from undergoing apoptosis. Given the lethal effects of BAD-BCL-X_L interaction, it is not surprising that BAD contains duplicate 14-3-3 binding sequences containing near-optimal and optimal matches to the consensus motifs to assure complete sequestration. PKB/AKT was recently shown to phosphorylate the RSRpSAP site of BAD (Datta et al., 1997; del Peso et al., 1997).

Our finding that peptides containing tandem binding motifs bind cooperatively to 14-3-3 is reminiscent of similar observations regarding cooperative binding to molecules containing tandem SH2 domains (Eck et al., 1996) and raises the possibility that 14-3-3 may sequester proteins containing multiple motifs such as BAD

Table 3. Predicted and/or Confirmed 14-3-3 Substrates

Protein	Predicted Binding Sites	Binding Confirmed
Mode 1 Binding		
Consensus: R-[S/Ar]-[+/Ar]-pSer-[LEAM]-Pro		
c-Raf-1	RST**S**^{259}TP, RSA**S**^{621}EP	Yes
A-Raf	RST**S**^{214}TP, RSA**S**^{582}EP	Yes
Cdc25a	RDS**S**^{191}EP,	Yes
Cdc25b	RPS**S**^{216}AP, RSP**S**^{309}MP, RSK**S**^{361}MP	Yes
Cdc25c	RSP**S**^{216}MP,	Yes
PKC-ϵ	RAA**S**^{380} SP	Yes
PCTAIRE-2	RAK**S**^{339}VP	Yes
mT	RSH**S**^{276}YP	Yes
Tyr hydroxylase	RHA**S**^{349}SP	Yes
Tryp hydroxylase	RHS**S**^{260}SP	Yes
A20	RSK**S**^{565}DP	Yes
BAD	RSH**S**^{112}YP, RSR**S**^{136}AP	Yes
Cb1	NRH**S**^{619}LP, RLG**S**^{639}TF	Yes
Mode 2 Binding		
Consensus: R-X-[Ar/S]-[+]-pSer-[LEAM]-Pro		
Cdc25a	RRIH**S**^{106}LP,	Yes
Cdc25b	RRFQ**S**^{136}MP,	Yes
PKCγ	RCVR**S**^{145}VP,	Yes
IRS-1	RPTR**S**^{975}VP	Yes
BCR	RASA**S**^{95}RP	Yes
K8 keratin	RSYT**S**^{27}GP	Yes
c-fes	RQYG**S**^{270}AP, RPKF**S**^{440}LP	No
Clathrin heavy chain	RRFQ**S**^{403}VP	No
Clathrin assembly prot.	RLYR**T**^{179}SP	No

Whenever possible, sequences are for human proteins. The designation of confirmed binding indicates only that the protein is known to interact with 14-3-3. Specific phosphorylation sites mediating 14-3-3 interaction have been identified only for members of the raf family, Cdc25c, Cbl, and BAD.

through a tight bidentate interaction within a single 14-3-3 dimer.

Furthermore, the cooperative nature of the binding can allow proteins containing tandem sequences to bind in cases where neither sequence alone is sufficient. This appears to be the case with Cbl, where neither of the two motifs implicated in 14-3-3 binding, NRHpSLP and RLGpSTF, individually allows interactions with 14-3-3, but the presence of both motifs confers stable binding (Liu et al., 1997).

In summary, we believe the nature of 14-3-3 interaction is determined by the extent to which the binding motif matches the optimal consensus sequence. This, in turn, determines if the role of 14-3-3 is to act as a sequestering molecule, a chaperone, or an adaptor. Whether this mode of sequence-dependent kinetic regulation, varying gradually from a sequestration-like to an adaptor-like function, also applies to other signaling modules such as SH2, SH3, and PTB-domain interactions, remains to be explored.

Experimental Procedures

Peptide Libraries

Phosphoserine-oriented degenerate peptide libraries of general sequence Met-Ala-Xxx-Xxx-Xxx-pSer-Xxx-Xxx-Xxx-Ala-Lys-Lys, theoretical degeneracy (td) = 4.7×10^7; Met-Ala-Xxx-Xxx-Xxx-Xxx-pSer-Xxx-Pro-Xxx-Xxx-Ala-Lys-Lys, td = 8.9×10^8; Met-Ala-Xxx-Xxx-Xxx-Arg-Xxx-Xxx-Arg-pSer-Xxx-Pro-Ala-Lys-Lys, td = 4.7×10^7; Met-Ala-Xxx-Xxx-Arg-Xxx-Xxx-pSer-Xxx-Pro-Ala-Lys-Lys, td = 2.5×10^6; and Met-Ala-Arg-Ser-Xxx-pSer-Xxx-Xxx-Ala-Lys-Lys, td = 6.9×10^3 were synthesized using N-α-FMOC-protected amino acids and standard BOP/HOBt coupling chemistry. Xxx represents all amino acids except cysteine.

14-3-3 Proteins

GST fusions of human β, η, σ, and S. cerevisiae Bmh1 and Bmh2 14-3-3s and MBP fusions of human τ, ζ, and ϵ 14-3-3s were generated by PCR amplification and cDNA cloning into pGEX 4T and pMalC2 vectors as previously described (Jones et al., 1995). Expression constructs were induced in late-log phase E. coli DH5α or DH10β by addition of 0.4 mM IPTG for 3–5 hrs at 37°C. Nonfusion 14-3-3 human ζ protein for 14-3-3/phosphopeptide cocrystallization was expressed and purified as described previously (Jones et al., 1995).

Library Screening

Fusion proteins (1–1.5 mg) bound to GST or Amylose beads were packed in small columns and incubated with 0.5–1.2 mg of the peptide library mixture for 10 min at room temperature in PBS containing 25 mM NaF, 100 μM Na_3VO_4, and 1% Triton X-100. Unbound peptides were removed by rapid washing (Songyang et al., 1993), and bound peptides eluted with 30% acetic acid for 10 min at room temperature, dried overnight on a Speed-Vac apparatus, resuspended in H_2O, and sequenced on an Applied Biosystems model 477A protein sequencer.

Preference values for amino acid selection were determined by comparing the relative abundance of each amino acid at a particular sequencing cycle (i.e., mol percentage) in the recovered peptides to that of each amino acid in the original peptide library mixture at the same position.

Surface Plasmon Resonance Measurements

Binding experiments were performed using a Biacore2000 instrument (Jonsson et al., 1991; 1993). Nonbiotinylated phosphopeptides (30 μl of 0.8 mM solutions) were immobilized on CM-5 sensor chips using EDC/NHS coupling chemistry as described by the manufacturer. Biotinylated phosphopeptides (20 μl of 1–2 μg/ml solutions)

were coupled to streptavidin-coated sensor chips, and underivitized sites blocked using 50 μM biotin. For kinetic measurements, 14-3-3η (50 nM–4 μM) was passed over the derivitized sensor chips in HEPES-buffered saline (pH 7.5) containing 0.005% Tween 20 at flow rates of 10–20 μl/min. The off-rate K_{off} was determined by analysis of the initial phase of the dissociation curves, and the on-rate K_{on} determined from the linear initial portion of the binding slope dR/dt by analyzing a range of protein concentrations with the Biaevaluation software.

Solution-inhibition assays were performed as recommended by the manufacturer. In brief, 40 μl of a 1.5 mM solution of c-raf-1 pSer-259 peptide was coupled to a CM-5 sensor chip and calibration curves of initial binding rate generated using low 14-3-3 protein concentrations. Under these conditions, 14-3-3 binding to the sensor chip is limited by mass-transport kinetics. 14-3-3 concentrations between 25 and 250 nM gave initial binding rates that varied linearly with concentration. At a selected 14-3-3 concentration, the protein was incubated with varying amounts of competing peptides for 1 hr at room temperature prior to injection of the entire peptide/protein mixture over the sensor-chip surface. The initial rate of binding, dR/dt_{init}, which indicates the amount of 14-3-3 not complexed to the inhibitor peptides, was plotted as a function of competing peptide concentration, and the K_i values corresponding to a 50% reduction in binding rate determined.

Crystallization and Data Collection

Initial crystals were grown at 4°C in hanging drops by vapor diffusion using equal amounts of protein–peptide complex (protein:peptide ratio 1:2) at 11.5 mg/ml in 20 mM Tris HCl (pH 7.5), 1mM EDTA, 1 mM DTT with reservoir solution containing 100 mM MES (pH 6.2), 20 mM $MgCl_2$, 20% isopropanol, and 15% PEG 4000. These crystals were substantially improved by micro- and macroseeding into a preequilibrated solution (2–3 days) made up with a reservoir solution containing 100 mM MES (pH 6.2), 20 mM $MgCl_2$, 14% isopropanol, and 12% PEG 4000. Crystals grew up to typical sizes of 60 × 70 × 90 μm^3 within 4–6 days and belonged to space group $P2_12_12_1$ (a = 68.6 Å, b = 71.9 Å, and c = 131.2 Å, with two complexes per asymmetric unit and the unit cell contains 56% solvent).

Diffraction datasets were collected from single crystals at 100°K using an Oxford Cryosystems device. Crystals were prepared for flash cooling by stepwise transfer (10 min per step) in mother liquor made up to 5%, 10%, and 20% glycerol. A native dataset to 2.6 Å was collected at station 5.2R at Trieste on a large MAR image detector. Data were processed with DENZO and SCALEPACK (Otwinowski, 1993), all subsequent calculations being performed with the CCP4 program suite (CCP4, 1994). The final dataset (R_{merge} = 5.6%) is 86% complete in the resolution range 15–2.6 Å.

Structure Determination

The structure of the 14-3-3ζ:phosphopeptide complex was solved by molecular replacement (Amore, CCP4), using the 14-3-3τ dimer as a starting model. Rotation/translation searches with subsequent rigid-body refinement were performed using data between 8 and 3.0 Å, yielding a single, unambiguous solution (R = 40%, correlation coefficient 0.624). Electron density maps calculated using phases derived from this model were averaged according to the local 2-fold axis. These 2-fold averaged phases were then included as additional restraints in subsequent positional refinement using REFMAC (CCP4, 1994). $2F_o$-F_c and F_o-F_c fourier maps showed clear density for the phosphopeptide, which was built using "O" (Jones et al., 1991). Refinement resulted in a crystallographic R factor of 24.6% (R_{free} = 29.7%) for all data between 15 and 2.6 Å with a model consisting of 454 residues of the zeta dimer, two phosphopeptides and 48 solvent molecules.

Acknowledgments

We thank Mike Berne for peptide synthesis and sequencing; Bing Xiao for further refinement of the 14-3-3τ structure; Zhou Songyang and Leslie Stolz for technical advice; the staff at Trieste for beamline assistance; and Guy G. Dodson for enthusiastic support throughout this work. *Bmh1* and *Bmh2* cDNAs were the kind gifts of Daniel Gelperin and Sandra Lemmon. The ζ 14-3-3/MBP construct was the kind gift of Paul Rose and Thomas M. Roberts. This research was supported, in part, by NIH Grant GM56203 (L. C. C.). M. B. Y. is funded as a Physician-Scientist Postdoctoral Fellow from the Howard Hughes Medical Institute, and K. R. is funded by an EEC TMR fellowship. S. V. is the recipient of a Human Frontier LTF.

Received October 1, 1997; revised November 12, 1997.

References

Aitken, A. (1996). 14-3-3 and its possible role in co-ordinating multiple signaling pathways. Trends Cell Biol. *6*, 341–347.

Aitken, A., Howell, S., Jones, D., Madrazo, J., and Patel, Y. (1995a). 14-3-3 α and δ are the phosphorylated forms of Raf-activating 14-3-3 β and ζ. J. Biol. Chem. *270*, 5706–5709.

Aitken, A., Howell, S., Jones, D., Madrazo, J., Martin, H., Patel, Y., and Robinson, K. (1995b). Post-translationally modified 14-3-3 isoforms and inhibition of protein kinase C. Mol. Cell. Biochem. *149*, 41–49.

Bonnefoy-Berard, N., Liu, Y.-C., von Villebrand, M., Sung, A., Elly, C., Mustelin, T., Yoshida H., Ishizaka, K., Altman, A. (1995). Inhibition of phosphoinositol 3-kinase activity by association with 14-3-3 proteins in T cells. Proc. Natl. Acad. Sci. USA *92*, 10142–10146.

Campbell, K.S., Ogris, E., Burke, B., Su, W., Auger, K.R., Druker, B.J., Schaffhausen, B.S., Roberts, T.M., and Pallas, D.C. (1994). Polyoma middle tumor antigen interacts with SHC protein via the NPTY (Asn-Pro-Thr-Tyr) motif in middle tumor antigen. Proc. Natl. Acad. Sci. USA *91*, 6344–6348.

Campbell, K.S., Auger, K.R., Hemmings, B.A., Roberts, T.M., and Pallas, D.C. (1995). Identification of regions in polyomavirus middle T and small t antigens important for association with protein phosphatase 2A. J. Virol. *69*, 3721–3728.

Carson, M. (1991). Ribbons 2.0. J. Appl. Crystallogr. *24*, 958–961.

CCP4. (1994). The CCP4 suite: programs for protein crystallography. Acta Crystallogr. *D50*, 760–763.

Courtneidge, S.A., and Smith, A.E. (1984). The complex of polyoma virus middle-T antigen and pp60c-src. EMBO J. *3*, 585–591.

Craparo, A., Freund, R., and Gustafson, T.A. (1997). 14-3-3 (ϵ) interacts with the insulin-like growth factor I receptor and insulin receptor substrate I in a phosphoserine-dependent manner. J. Biol. Chem. *272*, 11663–11669.

Datta, S.R., Dudek, H., Tao, X., Masters, S., Fu, H., Gotoh, Y., and Greenberg, M.E. (1997). AKT phosphorylation of BAD couples survival signals to the cell-intrinsic death machinery. Cell *91*, 231–241.

del Peso, L., Gonzalez-Garcia, M., Page, C., Herrera, R., and Nunez, G. (1997). Interleukin-3-induced phosphorylation of BAD through the protein kinase Akt. Science *278*, 687–689.

DuBois, T., Rommel, C., Howell, S., Steinhussen, U., Soneji, Y., Morrice, N., Molling, K., Aitken, A. (1997). 14-3-3 is phosphorylated by casein kinase 1 on residue 233. Phosphorylation at this site in vivo regulates Raf–14-3-3 interaction. J. Biol. Chem. *272*, 2882–2888.

Eck, M.J., Pluskey S., Trub, T., Harrison, S.C., and Shoelson, S.E. (1996). Spatial constraints on the recognition of phosphoproteins by the tandem SH2 domains of the phosphatase SH-PTP2. Nature *379*, 277–280.

Esnouf, R.M. (1997). An extensively modified version of MolScript that includes greatly enhanced coloring capabilities. J. Mol. Graph. *15*, 133–138.

Feng, S., Chen, J.K., Yu, H., Simon, J.A., and Schreiber, S.L. (1994). Two binding orientations for peptides to the Src SH3 domain: development of a general model for SH3-ligand interactions. Science *266*, 1241–1247.

Freed, E., Symons, M., Macdonald, S.G., McCormick, F., and Ruggieri, R. (1994). Binding of 14-3-3 proteins to the protein kinase Raf and effects on its activation. Science *265*, 1713–1716.

Fu, H., Xia, K., Pallas, D.C., Cui, C., Conroy, K., Narsimhan, R.P., Mamon, H., Collier, R.J., and Roberts, T.M. (1994). Interaction of the protein kinase Raf-1 with 14-3-3 proteins. Science *266*, 126–129.

Irie, K., Gotoh, Y., Yashar, B.M., Errede, B., Nishida, E., and Matsumoto, K. (1994). Stimulatory effects of yeast and mammalian 14-3-3 proteins on the Raf protein kinase. Science *165*, 1716–1719.

Jones, T.A., Zhou, J.Y., Cowan, S.W., and Kjeldgaard, M. (1991). Improved methods for building protein models in electron density maps and the location of errors in these models. Acta Crystallogr. *A47*, 110–119.

Jones, D.H.A., Martin, H., Madrazo, J., Robinson, K.A., Nielsen, P., Roseboom, P.H., Patel, Y., Howell, S.A., and Aitken, A. (1995). Expression and structural analysis of 14-3-3 proteins. J. Mol. Biol. *245*, 375–384.

Jonsson, U., Fagerstam, L., Ivarsson, B., Johnsson, B., Karlsson R., Lundh, K., Lofas, S., Persson, B., Roos, H., Ronnberg, I., et al. (1991). Real-time biospecific interaction analysis using surface plasmon resonance and a sensor chip technology. Biotech. *11*, 620–627.

Jonsson, U., Fagerstam, L., Lofas, S., Sternberg, E., Karlsson, R., Frostell, A., Markey, F., and Schindler F. (1993). Introducing a biosensor-based technology for real-time biospecific interaction analysis. Ann. Bio. Clin. *51*, 19–26.

Leffers, H., Madsen, P., Rasmussen, H.H., Honore, B., Andersen, A.H., Walbum, E., Vandekerchkhove, J., and Celis, J.E. (1993). Molecular cloning and expression of the transformation sensitive epithelial marker stratifin. J. Mol. Biol. *231*, 982–998.

Liao, J., and Omary, M.B. (1996). 14-3-3 proteins associate with phosphorylated simple epithelial keratins during cell cycle progression and act as a solubility cofactor. J. Cell Biol. *133*, 345–357.

Lim, W.A., Richards, F.M., and Fox, R.O. (1994). Structural determinants of peptide-binding orientation and of sequence specificity in SH3 domains. Nature *372*, 375–379.

Liu, D., Bienkowska, J., Petosa, C., Collier, R.J., Fu, H., and Liddington, R. (1995). Crystal structure of the ζ isoform of the 14-3-3 protein. Nature *376*, 191–194.

Liu, Y.-C., Elly, C., Yoshida, H., Bonnefoy-Berard, N., and Altman, A. (1996). Activation-modulated association of 14-3-3 proteins with Cbl in T cells. J. Biol. Chem. *271*, 14591–14595.

Liu, Y.-C., Liu, Y., Elly, C., Yoshida, H., Lipkowitz, S., and Altman, A. (1997). Serine phosphorylation of Cbl induced by phorbol ester enhances its association with 14-3-3 proteins in T cells via a novel serine-rich 14-3-3-binding motif. J. Biol. Chem. *272*, 9979–9985.

Meller, N., Liu, Y.-C., Collins, T.L., Bonnefoy-Berard, N., Baier, G., Isakov, N., and Altman, A. (1996). Direct interaction between protein kinase C θ (PKCθ) and 14-3-3τ in T cells: 14-3-3 overexpression results in inhibition of PKC θ translocation and function. Mol. Cell. Biol. *16*, 5782–5791.

Merritt, E.A., and Murphy, M.E.P. (1994). Raster3D Version 2.0, a program for photorealistic molecular graphics. Acta Crystallogr. *D50*, 869–873.

Moorhead, G., Douglas, P., Morrice, N., Scarabel, M., Aitken, A., and MacKintosh, C. (1996). Phosphorylated nitrate reductase from spinach leaves is inhibited by 14-3-3 proteins and activated by fusicoccin. Curr. Biol. *6*, 1104–1113.

Muslin, A.J., Tanner, J.W., Allen P.M., and Shaw, A.S. (1996). Interaction of 14-3-3 with signaling proteins is mediated by the recognition of phosphoserine. Cell *84*, 889–897.

Nicholls, A., Sharp, K.A., and Honig, B. (1991). Protein folding and association: insights from the interfacial and thermodynamic properties of hydrocarbons. Proteins, Struct. Funct. Genet. *11*, 281–296.

Nishikawa K., Toker, A., Johannes, F.-J., Songyang, Z., and Cantley, L.C. (1997). Determination of the specific substrate sequence motifs of protein kinase C isozymes. J. Biol. Chem. *272*, 952–960.

Otwinowski, Z. (1993). Oscillation data reduction program. In Data Collection and Processing, L. Sawyer, N. Isaacs, and S. Bailey, eds. (Warrington, UK: SERC Daresbury Laboratory), pp. 56–62.

Pallas, D.C., Fu, H., Haehnel, L.C., Weller, W., Collier, R.J., and Roberts, T.M. (1994). Association of polyomavirus middle tumor antigen with 14-3-3 proteins. Science. *265*, 535–537.

Pearson, R.B., and Kemp, B.E. (1991). Protein kinase phosphorylation site sequences and consensus specificity motifs: tabulations. Methods Enzymol. *200*, 63–81.

Peng, C.-Y., Graves, P.R., Thomas, R.S., Wu, Z., Shaw, A.S., and Piwnica-Worms, H. (1997). Mitotic and G2 checkpoint control: regulation of 14-3-3 protein binding by phosphorylation of Cdc25c on serine 216. Science, *277*, 1501–1505.

Rommel, C., Radziwill, G., Lovirc, J., Noeldeke, J., Heinicke, T., Jones, D., Aitken, A., and Moelling, K. (1996). Activated Ras displaces 14-3-3 protein from the amino terminus of c-Raf1. Oncogene *12*, 609–619.

Schulz, G.E., and Schirmer, R.H. (1979). Principles of Protein Structure. (New York: Springer-Verlag).

Songyang, Z., Shoelson, S.E., Chaudhuri, M., Gish, G., Pawson, T., Haser, W.G., King, F., Roberts, T., Ratnofsky, S., Lechleider, R.J., et al. (1993). SH2 domains recognize specific phosphopeptide sequences. Cell *72*, 767–778.

Stewart, D.E., Sarkar, A., and Wampler, J.E. (1990). Occurrence and role of *cis*-peptide bonds in protein structures. J. Mol. Biol. *214*, 253–260.

Toker A., Ellis, C.A., Sellers, L.A., and Aitken, A. (1990). Protein kinase C inhibitor proteins. Eur. J. Biochem. *191*, 421–429.

Vincenz, C., and Dixit, V.M. (1996). 14-3-3 proteins associate with A20 in an isoform-specific manner and function both as chaperone and adapter molecules. J. Biol. Chem. *271*, 20029–20034.

Wakui, H., Wright, A.P.H., Gustafsson, J.-A., and Zilliacus, J. (1997). Interaction of the ligand-activated glucocorticoid receptor with the 14-3-3η protein. J. Biol. Chem. *272*, 8153–8156.

Wheeler-Jones, C.P.D., Learmonth, M.P., Martin, H., and Aitken, A. (1996). Identification of 14-3-3 proteins in human platelets: effects of synthetic peptides on protein kinase C activation. Biochem. J. *315*, 41–47.

Whitman, M., Kaplan, D.R., Schaffhausen, B., Cantley, L., and Roberts, T.M. (1985). Association of phosphatidylinositol kinase activity with polyoma middle-T competent for transformation. Nature *315*, 239–242.

Xiao, B., Smerdon, S.J., Jones, D.H., Dodson, G.G., Soneji, Y., Aitken, A., and Gamblin, S.J. (1995). Structure of a 14-3-3 protein and implications for coordination of multiple signaling pathways. Nature *376*, 188–191.

Zha, J., Harada, H., Yang, E., Jockel, J., and Korsmeyer, S.J. (1996). Serine phosphorylation of death agonist BAD in response to survival factor results in binding to 14-3-3 not BCL-X_L. Cell *87*, 619–628.

Zhang, L., Wang, H., Liu, D., Liddington, R., and Fu, H. (1997). Raf-1 kinase and exoenzyme S interact with 14-3-3ζ through a common site involving lysine 49. J. Biol. Chem. *272*, 13717–13724.

Brookhaven DataBank Accession Number

The accession number for the structure reported in this paper is 14PS.